The effect of Mirazid (*Commiphora molmol*) on mitigating Brain damage caused by *Hymenolepiasis Nana: A* histochemical Evaluation

Biodiversity Research Journal, 2025,

volume 3, issue 1, 192-208

AUTHORS

Hanan T. Hamza,[1,2] and Mervat A. EL-Alfy[3]

AFFILLIATIONS

[1]Department of Biology, College of Science, Jouf University, P.O. Box: 2014, Sakaka, Saudi Arabia

[2]Department of Zoology, Faculty of Science for Girls, Al-Azhar University, Cairo, Eygpt

[3]Department of Biology, Faculty of Sciences, University of Bisha, P.O.Box:551, Bisha 61922, Saudi Arabia.

CORRESPONDENCE

maahmed@ub.edu.sa

SUBMISSION HISTORY

RECIVED: January 29, 2025

ACCEPTED: March 18, 2025

PUBLISHED: June 30, 2025

CITATION

Hamza, H T and EL-Alfy , M A. The effect of Mirazid (Commiphora molmol) on mitigating Brain damage caused by *Hymenolepiasis Nana: A histochemical Evaluation*. *Biodiversity Research Journal*, 2025, 3(**1**): 192-208.

ABSTRACT

Hymenolepiasis is the most prevalent tapeworm infection worldwide. While praziquantel is the primary treatment for *Hymenolepis nana* (H. nana), studies on albino rats have demonstrated its hepatotoxic, genotoxic, and carcinogenic effects. Mirazid (*Commiphora molmol*) has emerged as a safer and effective alternative for treating hymenolepiasis. This study aimed to investigate the Neuropathological alterations of *H. nana* infection in immunocompromised hosts. One hundred twenty male Swiss albino mice were divided into immunocompetent and immunocompromised groups by administering a dose of 8 mg/kg body weight (BW) of dexamethasone sodium phosphate subcutaneously for seven days in order to avoid edema or unintended weight gain. At different post-infection time points (the experimental mice were sacrificed on days 15 and 21 post-infection for determination of which drug gives more effect (cure rate)), mice were sacrificed, and their brain tissues were subjected to histochemical and histological analyses. The findings revealed significant histopathological alterations in the brains of immunosuppressed mice. Immunocompetent groups showed improvements in brain histopathology when praziquantel (PZQ)-treated mice were compared to those given Mirazid oleoresin extract at a dose of 10 mg/kg/BW for six days after infection. Unlike what occurred in the immunodeficient group, where there was an increase in histological alterations. Hence, histopathological alterations in the brains of infected mice were progressive and exacerbated under immunosuppressive conditions, correlating with increased cerebral parasite burden. Histochemical staining (e.g., hematoxylin and eosin) revealed significant Neuropathological changes. However, further research is needed to determine whether these alterations are directly caused by the presence of the parasite or by host immune responses to infection and treatment.

KEYWORDS: *Hymenolepis nana,* immunosuppression, praziquantel, Mirazid (*Commiphora molmol*)

INTRODUCTION

Neurocysticercosis (NCC) is a significant global cause of morbidity, resulting from a helminthic infection of the central nervous system (CNS) by the larval stage of Taenia solium (cysticercus), as seen in H. nana infection in immunocompromised hosts (Orozco et al., 2018). Among human cestode infections, Hymenolepis nana (dwarf tapeworm) is the most prevalent, primarily affecting children due to poor hygiene and sanitation.

Estimates suggest that between 50 and 75 million individuals worldwide are infected with *H. nana*, with high prevalence rates in tropical regions, such as Egypt, Africa, Asia, and parts of southern and eastern Europe (El-Gammal et al., 1995 & Bagayan et al., 2015). Individuals with weakened immune systems are particularly susceptible, as the parasite can proliferate within their bodies through autoinfection (WHO, 2013). H. nana is mostly spread by the fecal-oral route and does not need an intermediary host for its life cycle, in contrast to *Hymenolepis diminuta*. Infection typically occurs through ingestion of contaminated eggs, leading to intestinal colonization. While Hymenolepis infections are often asymptomatic, the larval stages may trigger immunological responses. *H. nana* has also been studied for its potential immunomodulatory effects, with research suggesting it may play a role in mitigating colitis (Bhosale, 2022). Diagnosis is primarily based on microscopic detection of eggs in fecal samples. Praziquantel remains the treatment of choice, while proper hygiene practices are fundamental to preventing transmission. Despite its typically asymptomatic nature, *H. nana* infection can lead to severe CNS complications, especially in immunocompromised hosts, children, and those with ongoing illnesses (Bhosale, 2022). Rodents, especially rats and mice, serve as natural reservoirs for *H. nana*, with reported prevalence rates of 33.93% in rats and 32% in mice (Pinto et al., 1994; Gudissa et al., 2011).

Transmission occurs through the ingestion of embryonated eggs or arthropods carrying cysticercoids, This may come from tainted food, water, or direct interaction. When the eggs are consumed, hexacanth larvae are released, which penetrate the intestinal mucosa, enter the bloodstream, and migrate to various tissues, including the CNS. Once in the brain, the larvae often localize within the parenchyma, subarachnoid space, or ventricular system, developing into mature cysticercoids that provoke neuroinflammatory responses and neurological impairments (Cho et al., 2009). Astrocytes and microglia play critical roles in maintaining CNS homeostasis and responding to neural damage. Astrocytes contribute to gliosis, a reparative process that involves cytokine release and regulation of the blood-brain barrier, whereas microglia support axonal integrity and synaptic remodeling in both normal and damaged neural environments (Nimmerjahn et al., 2005; Tremblay et al., 2010; Paolicelli et al., 2011; Schafer et al., 2013). Ma et al. (2022) found that 132-hydroxy-(132-S)-pheophytin a from *Leucaena leucocephala* effectively reduced tapeworm infection in mice by lowering worm count, egg production, and enhancing immune response. Although the brain lacks traditional lymphatic vessels, alternative pathways, such as cerebrospinal fluid drainage to cervical lymph nodes (CLNs), help regulate immune responses. The neurovascular unit (NVU) further acts as a selective barrier, limiting leukocyte infiltration into the brain parenchyma (Bechmann & Woodroofe, 2014; Dyrna et al., 2013). Due to their broad-spectrum antiparasitic properties and minimal adverse effects compared to conventional chemotherapeutics, plant-derived essential oils have garnered interest as alternative treatments for parasitic infections (Etewa & Abaza, 2011). The need for such alternatives is reinforced by concerns regarding the hepatotoxic, genotoxic, and potentially carcinogenic effects of widely used anthelmintics like praziquantel, particularly in immunosuppressed individuals (Omar et al., 2005). Experimental models using dexamethasone sodium phosphate to induce immunosuppression highlight the need for effective therapeutic strategies in managing H. nana infections (Medeiros et al., 2010).

MATERIALS AND METHODS

Animals

Male Swiss albino mice, weighing approximately 20–25 g (±2 g), were bred and maintained at the Theodore Bilharz Research Institute (TBRI), Egypt. All experiments followed internationally recognized guidelines for animal research and ethical standards (Nessim et al., 2000). They were obtained from the Biology Supply Center of the Theodor Bilharzia Research Institute (TBRI) in Giza, Egypt. They were housed at a consistent room temperature of 22 ±2 ○C in the TBRI animal housing. The standard food and water were available to the animals without restriction. All animal care and procedures were carried out in compliance with global ethical standards after receiving approval from TBRI's institutional ethics committee. The Department of Zoology, Faculty of Science (Girls), Al-Azhar University, conducted histopathological and quantitative image analysis."

Experimental Design

A total of 120 male albino mice were divided into two main groups:

1.**Immunocompetent Groups**

- **Group 1 (Infected Untreated Control)**: Infected with *Hymenolepis nana* but untreated.

- **Group 2** According to Massoud et al. (2007), mice were infected and given oral treatment with Mirazid (Pharco, Egypt) at a dose of 10 mg/kg/BW for six days after infection. Comparing the effects of Mirazid (Commiphora molmol), a herbal remedy, to PZQ (the conventional treatment) in immunocompetent and immunocompromised patients albino mice with the infection. Mirazid is superior to PZQ in treating H. nana infections, with significant improvements in both biochemical and histopathological outcomes.

- **Group 3 (Praziquantel Treated)**: A single dosage of praziquantel (EPICO, Egypt) at a dose of 25 mg/kg/BW was administered orally to infected mice on the tenth day after infection, as per Bhat-tacharya et al. (2003).

. 2.**Immunocompromised Groups**

- **Group 4 (Cortisone and Infected)**: Injected with dexamethasone sodium phosphate and infected with *H. nana* (250 eggs/mouse).

- **Group 5 (Cortisone, Infected, and Mirazid Treated)**: Injected with dexamethasone sodium phosphate, infected with *H. nana* (250 eggs/mouse), and treated with Mirazid (10 mg/kg body weight) orally for six days post-infection. Mirazid showed higher cure rates than PZQ. This plant extract also showed a notable decrease in fibrotic content.

- **Group 6 (Cortisone, Infected, and Praziquantel Treated)**: Injected with dexamethasone sodium phosphate, infected with *H. nana* (250 eggs/mouse), and treated with praziquantel (25 mg/kg body weight) orally on the 10th day post-infection.

The experimental mice were sacrificed on day 21 post-infection to assess the treatment efficacy (cure rate).

Stool Sample Collection

Stool samples infected with *H. nana* were collected from patients attending TBRI. Eggs were isolated and processed according to Macnish (2001). The suspension was centrifuged, and the infective eggs were washed with phosphate-buffered saline (PBS) to remove any residual salt.

Animal Infection Protocol

Mice were infected orally with 200–250 *H. nana* eggs using a tuberculin syringe connected to a polyethylene tube, ensuring the dose was directly delivered into the esophagus (Ito et al., 1991).

Drugs Used

Praziquantel (PZQ)

Praziquantel (Discocide), manufactured by the Egyptian International Pharmaceutical Industries Company (EPICO), was administered at a dose of 25 mg/kg body weight, dissolved in 10% dimethyl sulfoxide (DMSO) (Bhattacharya et al., 2003).

Dexamethasone Sodium Phosphate

Dexamethasone sodium phosphate (Amriya Pharm. Ind., Alexandria, Egypt) was administered subcutaneously at a dose of 8 mg/kg body weight daily for seven days (Medeiros et al., 2010). Immunosuppression is assessed indirectly by monitoring immunosuppressive drug levels in the blood, observing the patient's susceptibility to infections or toxic side effects, and sometimes through assays that measure the immune system's functional response. While direct measurement of the immune state is challenging, methods such as checking blood cell counts and immunoglobulin levels can indicate a defect. Newer techniques, on the other hand, examine virus-specific T cells (Tvis) or cytokine profiles from stimulated blood to assess individual immune function and the effects of drugs (Lversen, 2013).

Mirazid

Mirazid, an oleoresin extract from *Commiphora molmol* capsules (Pharco Pharmaceuticals Company, Alexandria, Egypt), was given orally starting six days after infection at a rate of 10 mg/kg body weight each day (Massoud et al., 2007b).

Histopathological Examination

The brain tissues were fixed in 20% neutral formalin, dehydrated in ascending grades of alcohol, cleared in xylene, and embedded in paraffin wax. Serial sections (5 μm) were prepared and stained using various histochemical techniques, including (H&E) General stain, Mallory's trichrome for collagen (Pearse, 1977), (PAS) for glycogen (Hotchkiss, 1948), bromophenol blue (Mazia et al., 1953), and Congo red (Sheehan & Hrapchak, 1980; Valle, 1986). Paraffin sections (4–5 μm) were stained with the Feulgen reaction, Mallory, bromophenol, Congo red, and PAS stains (for glycoproteins in neurodegeneration) (Suvarna et al., 2013). Sections that had been stained were checked for corresponding cellular, nuclear, and cytoplasmic structural reactivities.

Histopathology: Image Pro-Plus software (version 5.0) was used for image analysis. Images obtained from a digital camera were analyzed for quantitative measurements (Reedy & Kamboj, 2004).

Statistical Analysis: Data were expressed as means ± standard deviation (SD). Statistical significance was determined using one-way ANOVA, and differences were considered significant at $p < 0.05$. The SPSS software (version 10 for Windows) was used for statistical computations.

RESULTS

Brain examination showed marked histopathological changes in immunosuppressed mice. Mice infected with Hymenolepis nana showed improvements in their histological alterations., treated with praziquantel (PZQ), and compared with Mirazid oleoresin extract-treated groups in Immunocompetent groups; however, changes were observed in Immunocompromised groups. When comparing the two groups treated with PZQ, Mirazid, with the untreated groups, a statistically significant increase was shown (P <0.001).

Brain of mice from group G1, infected and untreated control group, showing a large focal hemorrhage area with disintegrated neurofibromas, faintly stained, and highly affected neurons. It also showed congestion of blood vessels and perivascular cuffing with mononuclear cells. Examination showed focal necrosis associated with glial cell infiltration. Most neurons are highly disorganized and faintly stained, with their nuclei significantly reduced, and are accompanied by destroyed and ruptured nanofibrous structures with highly dilated spaces in between them. Additionally, there are depressions of degenerated neurons and evidence of neuronal necrosis and neuronophagia, Fig. (1) (H&E x400).

Brains of G2 mice (infected and treated with Mirazid) showed neuronal necrosis, neuronophagia, perivascular cuffing, large, damaged areas with WBCs, hydrolyzed RBCs, and neurons with pyknotic (p) or karyolytic (k) nuclei and perineuronal spaces, Fig. (2) (H&E x400).

The brains of mice from group G3, Infected and treated with praziquantel, showed cellular edema. Most neurons contained highly atrophied and pyknotic (p) nuclei or karyolitic (k) ones. Additionally, there was necrosis of neurons and neuronophagia. Examination revealed necrosis of some neurons and neuronophagia, with no histopathological changes observed, Fig. (3) (H&E x400).

The brains of mice from group G4, Cortisone, and the infected group showed necrosis of neurons and focal hemorrhage, also showing highly ruptured and highly disintegrated neurofibrous tissue with highly congested and dilated blood vessels and focal gliosis. Examination showed necrosis of neurons and congestion of highly dilated and elongated cerebral blood vessels. It showed necrosis of neurons with dystrophic changes, including atrophied ones with highly widened pericellular spaces, completely destroyed cytoplasm and nuclei of the remnant ones and cellular organoids, with large hemorrhagic areas, containing RBCs and numerous WBCs, Fig. (4) (H&E x400).

Brain of mice from group G5 Cortisone, infected and Mirazid showing cellular oedema with highly dilated and congested of cerebral blood vessel with delaminated endothelial lining of it, also showed necrosis of neurons and neuronophagia, examination showed perivascular cuffing with mononuclear cells, with pyknotic nuclei, some degenerated neurons has karyolitic(k) with pericellular large empty spaces with dilated and elongated

blood capillary (by) and showed cellular oedema, completely destructed neurons with widened pericellular spaces and disintegrated of neurofibrous with complete loss of architecture brain tissues, also showed necrosis of neurons with faintly stained neurofibrous, Fig. (5) (H&E x400).

Brain of mice from group G6 Cortisone, infected and PZQ treated group showing focal necrosis associated with glial cells infiltration, most of neurons are highly atrophic with widened pericellular spaces with increased signs of pykinosis (p) or karyolitic and highly degenerated neurofibrous, also showed perivascular cuffing with mononuclear cells, with pyknotic nuclei, some degenerated neurons have karyolitic (k) with pericellular large empty spaces with dilated and elongated blood capillary (bv), and showed necrosis of neurons, Fig. (6) (H&E x400).

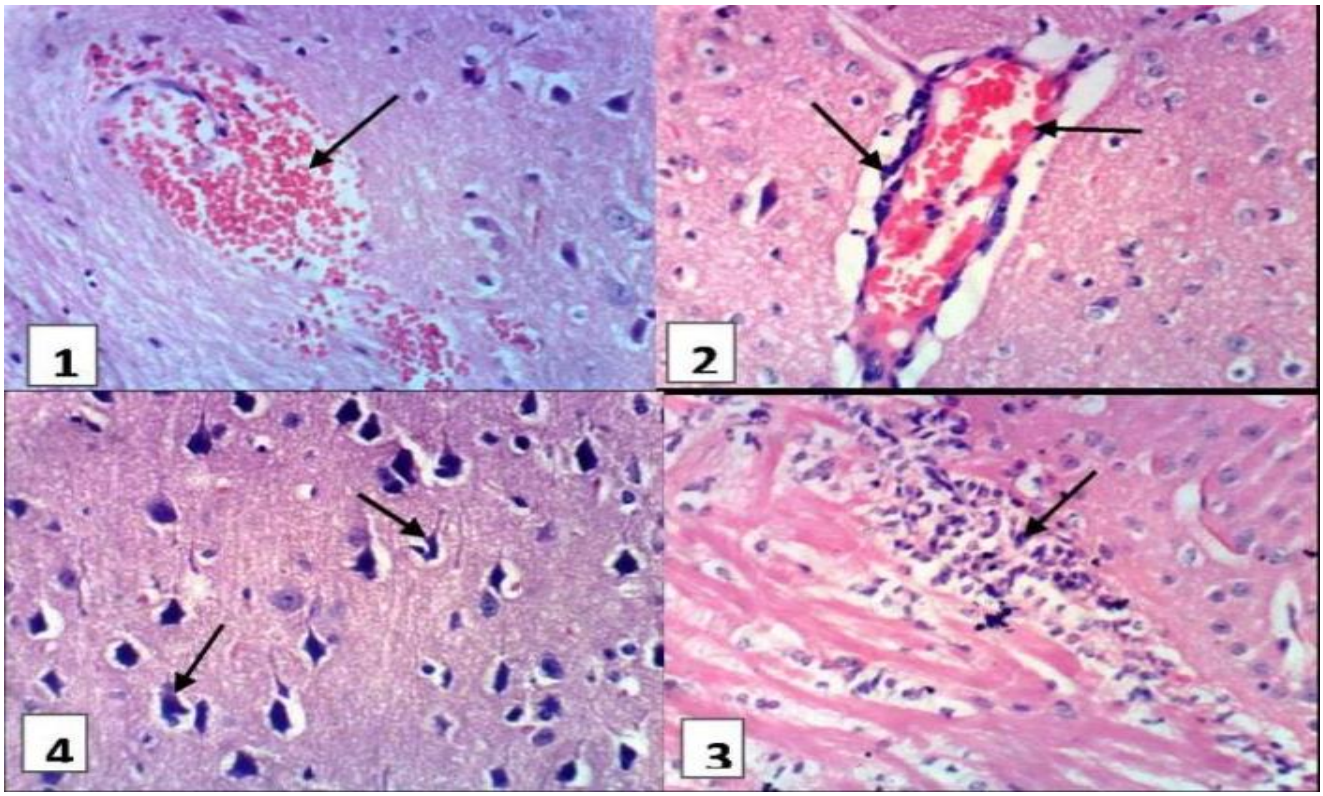

Figure 1. The brains of mice from group G1, the infected, untreated control group, show a large focal hemorrhagic area, with disintegrated neurofibromas and faintly stained, highly affected neurons (1). (2) This shows congestion of blood vessels, perivascular cuffing with mononuclear cells, and congested blood vessels. (3) This depicts focal necrosis associated with glial cell infiltration, where most neurons appear highly disturbed and faintly stained, their nuclei significantly reduced, with destroyed and ruptured nanofibers and highly dilated spaces between them. It also contains depressions from degenerated neurons. (4) This displays neuronophagia and neuronal necrosis (H & E x400).

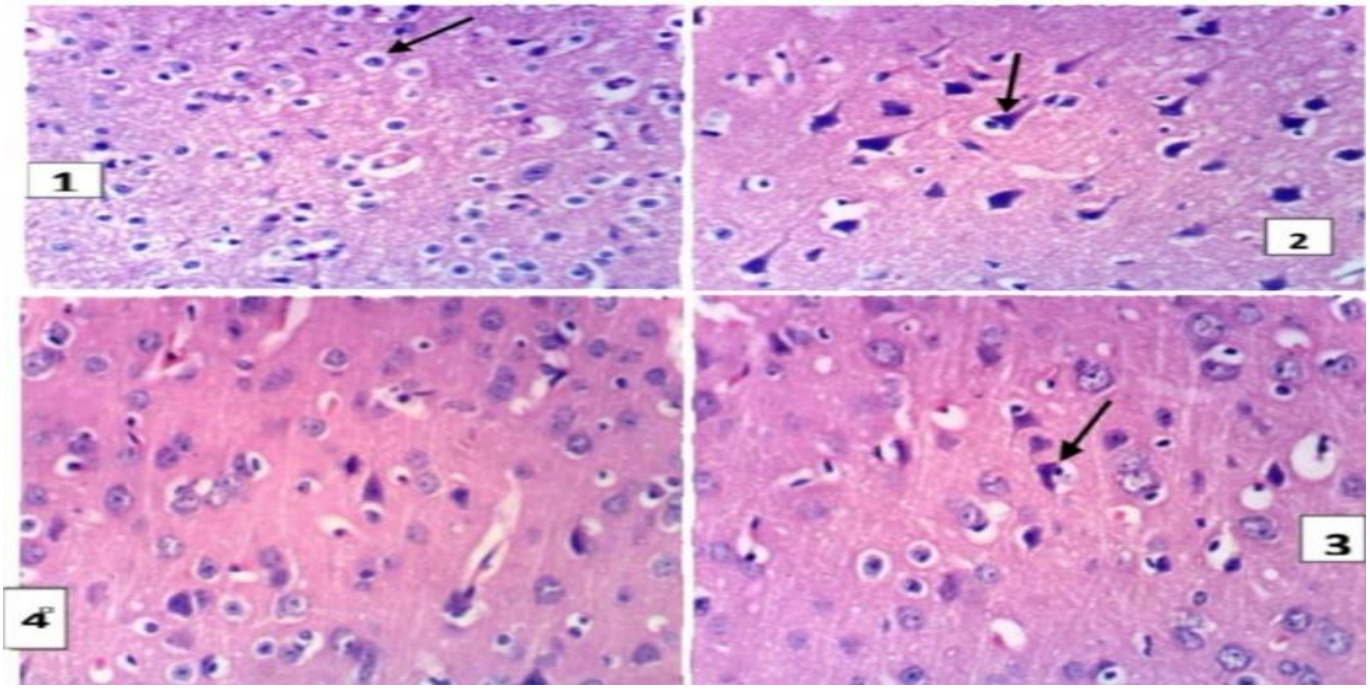

Figure 2. Brain of mice from group G3 Infected and treated with praziquantel showing cellular oedema, most of neurons contain highly atrophied and pyknotic (p) nuclei or karyolitic(k) ones (←) (1), (2) showing necrosis of neurons and neuronophagia, (3) demonstrating neuronophagia and some neuron necrosis(4) showing no histopathological changes (H & E x 400).

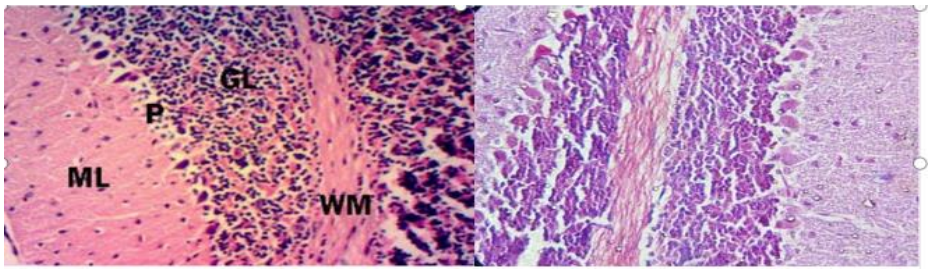

Typical appearance of a section of brain stain with (H & E x100 and x400).

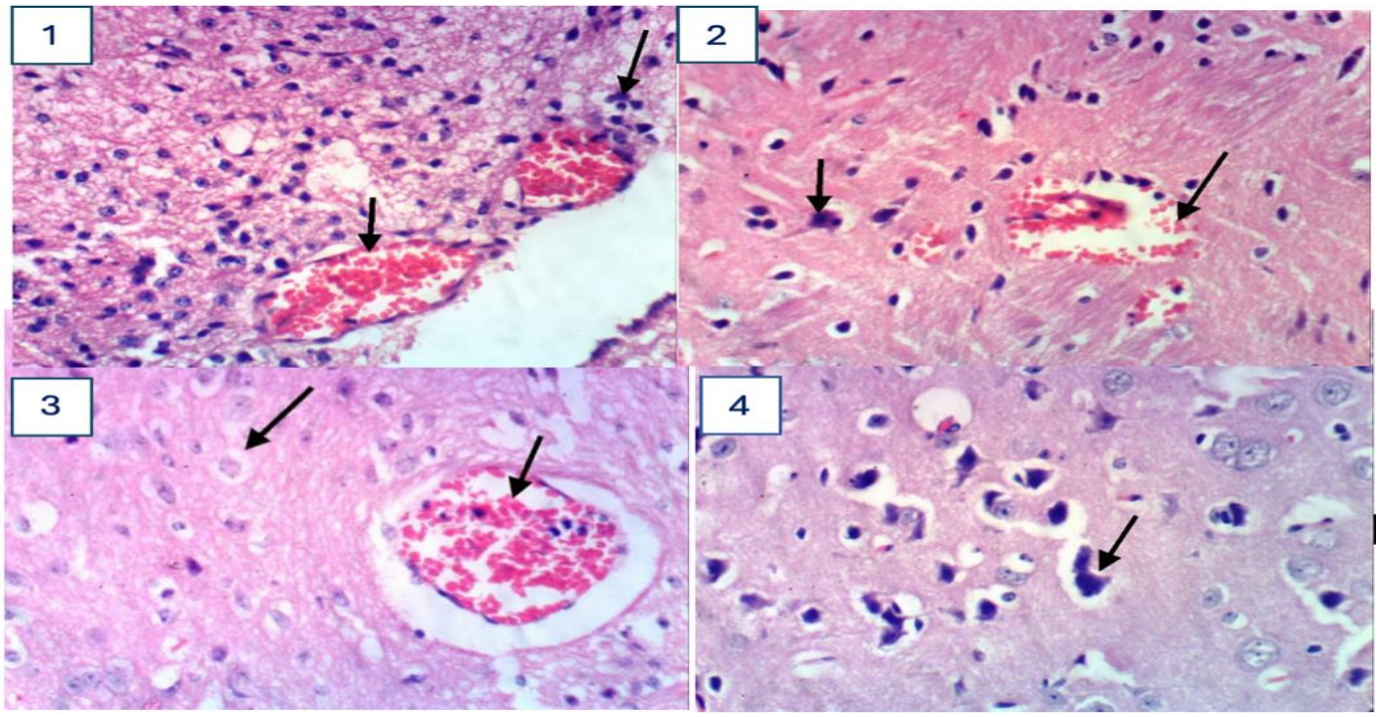

Figure 3. Brain of mice from group G4, Cortisone, and infected group showing necrosis of neurons and focal hemorrhage (1), (2) showing necrosis of neurons and congestion of highly dilated and elongated cerebral blood vessels. Additionally, the brains of mice from group G5 Cortisone, infected with Mirazid, exhibited cellular edema with highly dilated and congested cerebral blood vessels, a delaminated endothelial lining (3), and neuronal necrosis (←), accompanied by faintly stained neurofibers (4) (H&E x 400).

Histochemical Findings

Feulgen reaction, for nuclear DNA.

Almost all of the examined sections from different experimental groups showed normal nuclear reactivities, with a more reactive hippocampus cell in groups 2 and 4. Reactive glial and round cellular aggregates are seen in the vicinity of blood vessels and peri-ventricular areas in group 1. Focal reactive gliosis with prominent nuclei is observed in the group, Figs. (1,2).

Bromophenol, for cellular protein contents.

Brain tissue from the different experimental groups stained with bromophenol showed normal cellular, nuclear, and cytoplasmic protein contents in all cerebral and cerebellar structures of the control negative group (N) and in some cerebral and cerebellar structures of all infected-treated groups (G2-G6) (yellow arrows). A moderate depletion of cellular protein is observable in all infected-treated groups (G2-G6). The depletive reaction was more potent in the infected nontreated group (G1). Figs. (3,4).

PAS Stain for polysaccharides (glycogen and glycoprotein)

PAS staining is primarily used for detecting polysaccharides, including glycogen, glycoproteins, and glycolipids. Thus, this staining has been used to evaluate liver diseases associated with glycogen deposition, lung diseases caused by mucin abnormalities, and other conditions. However, the staining is rarely used for

histopathological analysis of brain tissues. Examined sections from the control negative group revealed an overall normal distribution of glycoprotein and glycolipid molecules in different cerebral and cerebellar structures. On the other hand, the treated groups (G1-G6) showed degenerative changes in neuronal, glial, and Purkinje cells, accompanied by increased deposition of glycoproteins and glycolipids, resulting in intense positive PAS staining. The reaction was more unmistakable and characteristic in group 1. Degenerated axons also intensely reacted positively. Demyelinated and vacuolated axons and neurons were negatively stained and assumed a paler color affinity. Figs. (5,6).

Congo red stain for cerebral amyloid-associated protein.

Amyloid is homogeneous and eosinophilic; the deposits are extracellular and may become sufficiently large to cause damage to surrounding tissues. When stained with Congo Red, amyloid exhibits birefringence in an apple-green color under the microscope, aided by polarizing lenses. In brain tissue, amyloid appears as extracellular plaques and intracellular neurofibrillary tangles (NFTs). Neurofibrillary tangles are abnormal accumulations of a protein called tau that collect inside neurons. Congo red-stained sections from control-negative rats were free of amyloid deposition. Large amounts of both extracellular bright red amyloid deposits and neurofibrillary tangles (abnormal protein deposition) were recorded in the larva migrants infected group (G1). On the other hand, variable amounts of amyloid deposits were seen in all treatment groups, with a minimal change in groups (5, 6). Figures 7,8.

5. Mallory For collagen fibers and other tissue features, use the Trichrome stain.

Mallory's trichrome is based on nuclear staining with carbol fuchsin and associated cytoplasmic staining with G-orange, as well as highly selective collagen staining with aniline blue. The selectivity of the method is based on the different degrees of chemical affinity of the dyes used for tissue macromolecules. The role of phosphomolybdic acid, in particular, is fundamental because it serves as a bridge between the tissue structures to which it selectively binds (collagen fibrils, cell membranes, etc.) and aniline blue (amphoteric dye). The other component of Mallory's trichrome, the orange G, which has no affinity for phosphomolybdic acid, stains the remaining structures (which are not linked to phosphomolybdic acid). Nuclei, neurofibrils, cartilage, and bone tissue: red. Collagen Fibers: Blue. Erythrocytes, myelin: golden yellow. Elastic fibers: pale pink-yellow or colorless. Examined tissue sections from the nervous tissue of control-free rats revealed negative deposition of collagen fibers. Sections from different infected-treatment regimens denoted axonal, neuropil, and neurofibrillary degenerative changes of variable internists with a golden yellow positive reaction to the remaining unaffected myelinated fibrils. No collagen deposition in any of the examined cases was recorded. Figs. (8).

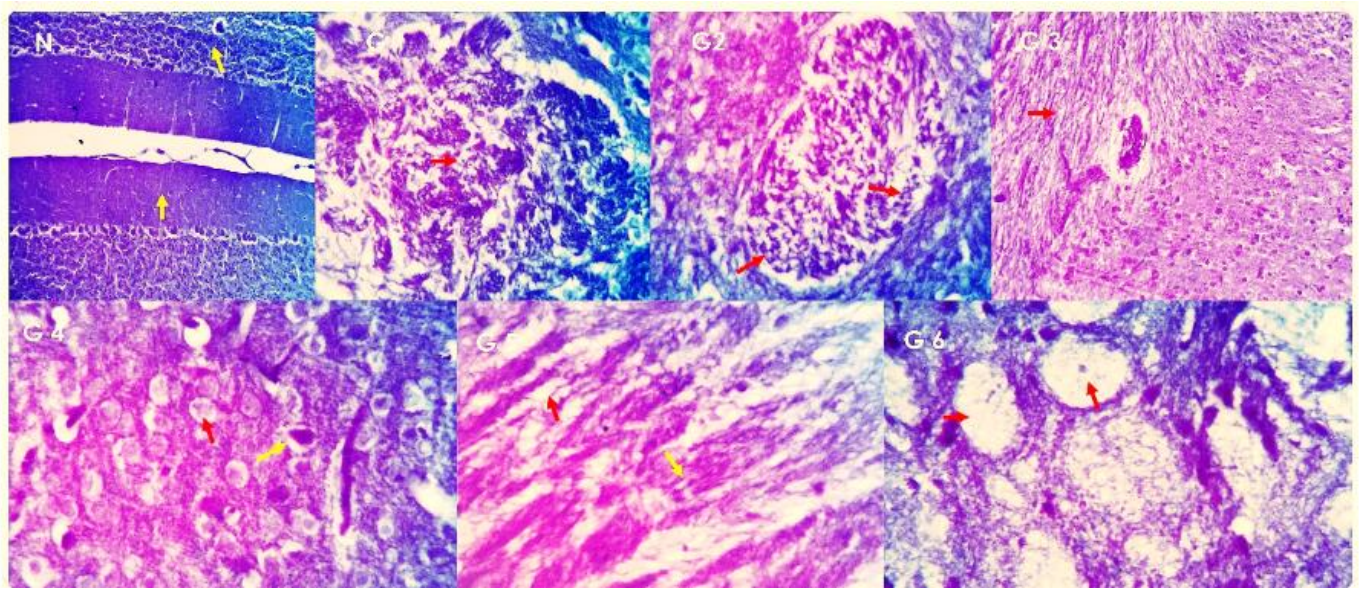

Figure 4. Photomicrographs from brain tissue of the different experimental groups stained by bromophenol stain, showing normal cellular nuclear and cytoplasmic protein contents in all cerebral and cerebellar structures of the control negative group (N) and some cerebral and cerebellar structures of all infected-treated groups (G2-G6) (yellow arrows). A moderate depletion of the cellular protein is observable in all infected-treated groups (G2-G6) (red arrows). The depletive reaction is more potent in the infected nontreated group (G1) (red arrows). (x 400).

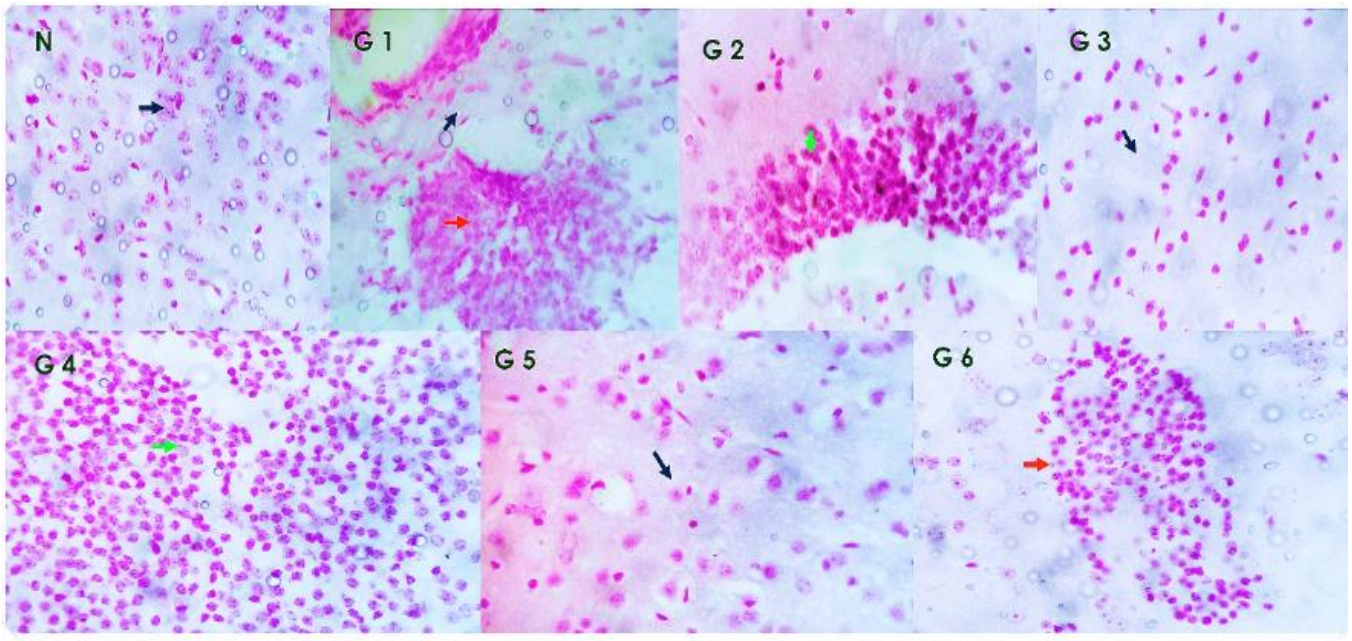

Figure 5. Photomicrographs of brain tissue from various experimental groups stained with Feulgen stain, depicting normal nuclear reactivities (dark blue arrows) alongside more reactive hippocampal cells in groups 2 and 4 (green arrows). Reactive glial cells and round cellular aggregates are seen near blood vessels and periventricular areas in group 1 (red arrow). Focal reactive gliosis with prominent nuclei is observed in group 6 (orange arrow). (x 400).

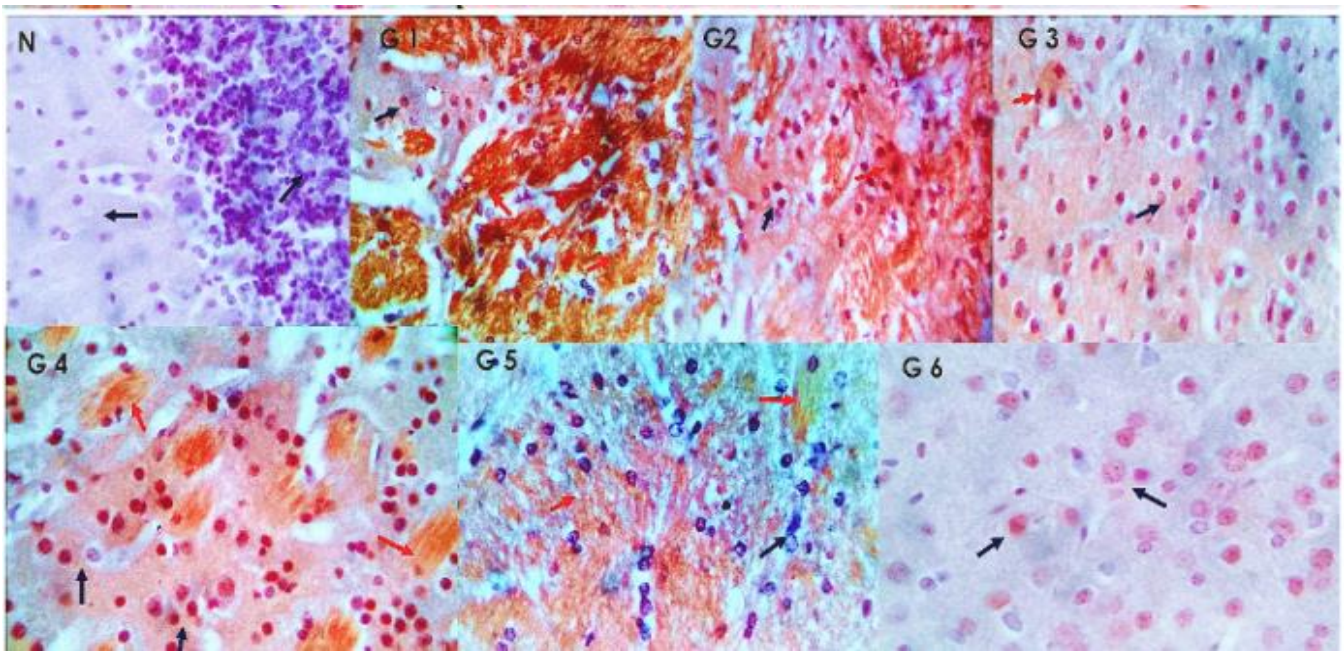

Figure 6. Photomicrographs from brain tissue of the different experimental groups stained by Congo red stain, showing amyloid-free tissue cells and neurofibrils in control negative rats (G 1)(dark blue arrows). Large amounts of both extracellular bright red amyloid deposits and neurofibrillary tangles (abnormal protein deposition) are seen in the larva migrants infected group (G 1) (red arrows). On the other hand, variable amounts of amyloid deposits are observable in all treatment groups, with minimal changes between groups (5, 6) (red arrows). Amyloid-free brain tissue is marked by dark blue arrows . (x 400).

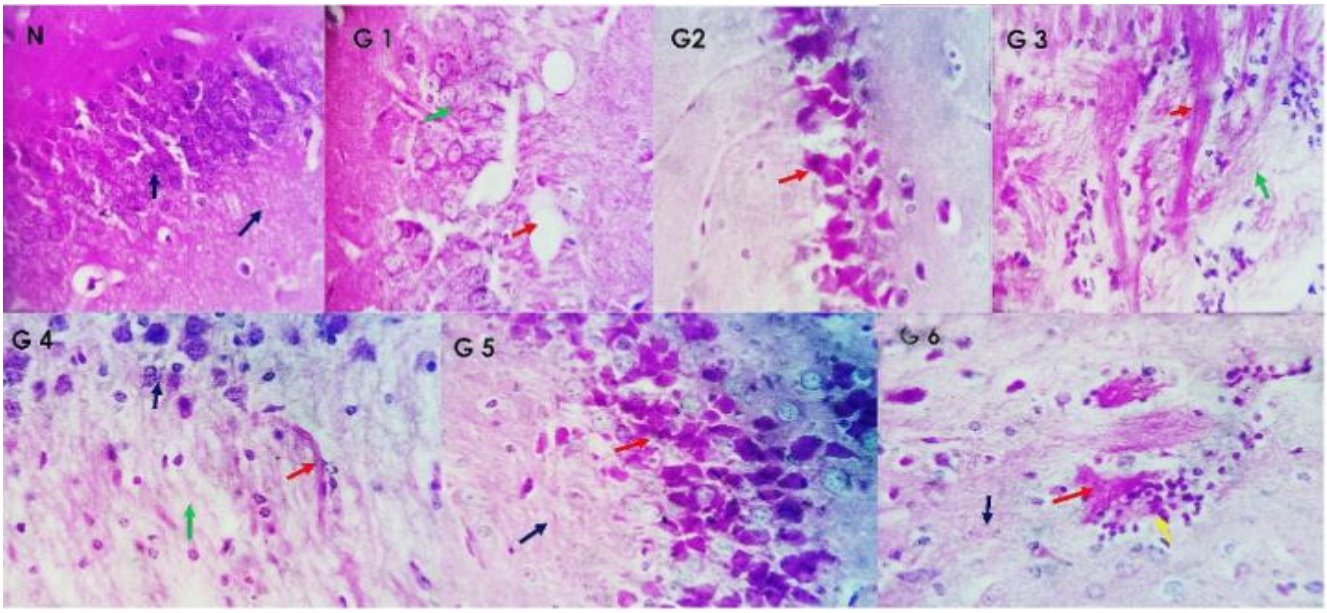

Figure 7. photomicrographs of the various experimental groups' brain tissue stained with Periodic Acid Schiff (PAS) dye,, showing overall normal distribution of the glycoprotein and glycolipid molecules in different cerebral and cerebrum structures (dark blue arrows). On the other hand, the treated groups (G1-G6) exhibit degenerative changes in neuronal, glial, and Purkinje cells, accompanied by increased deposition of glycoproteins and glycolipids, resulting in intense positive PAS staining (indicated by red arrows). The reaction

appears more straightforward and characteristic in group 1. Degenerated axons also appear intensely positively reacted (red arrows). Demyelinated and vacuolated axons and or neurons are negatively stained and assumed to have a paler color affinity (green arrows). (x 400).

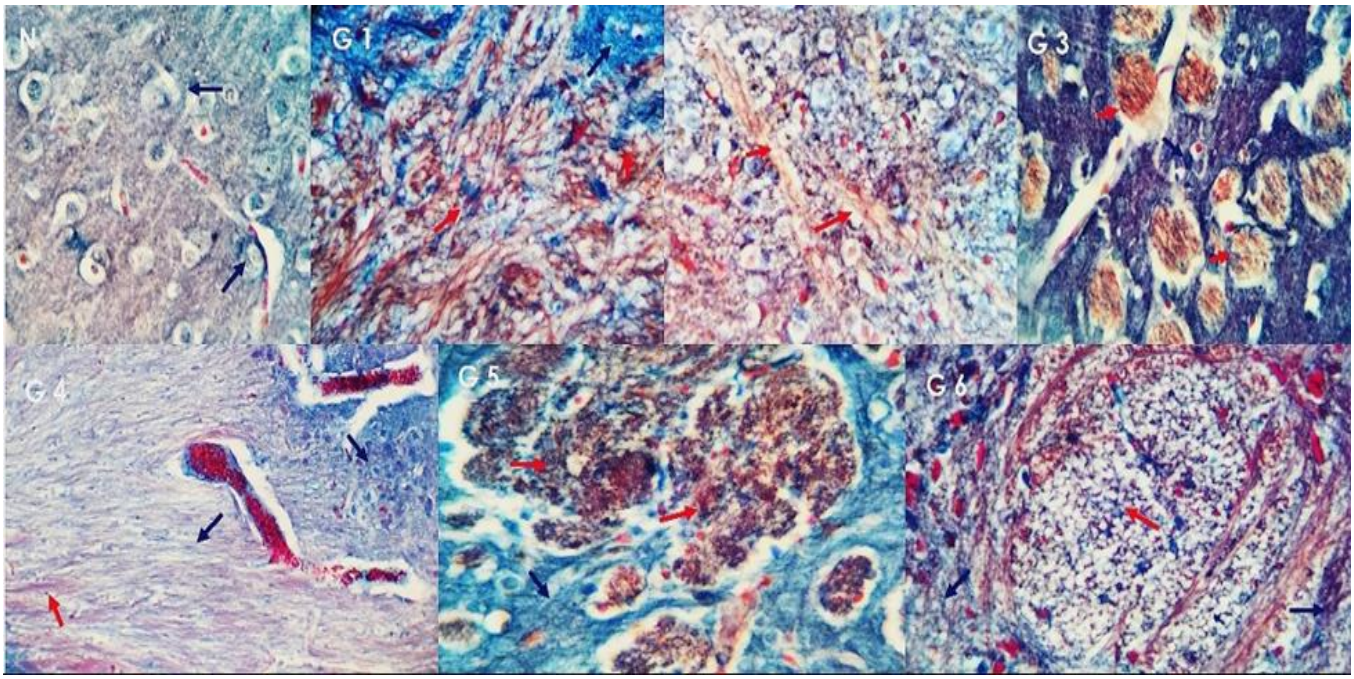

Figure 8. photomicrographs from brain tissue of the different experimental groups stained by Mallory trichrome stain, showing negative deposition of collagen fibers in control free rats (dark blue arrows). Sections from different infected treatment regimens exhibit axonal, neuropil, and neurofibrillary degenerative changes of variable intensity, accompanied by a golden yellow positive reaction in the remaining unaffected myelinated fibrils (red arrows). No collagen deposition is seen. Typical brain tissue structures marked by dark blue arrows. (x 400).

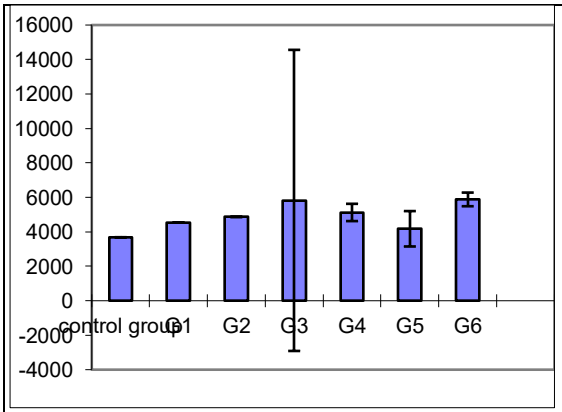

Histogram 1. Revealing the optical density values (mean±SD) of Cong red materials in the brains of mice of the different experimental groups.

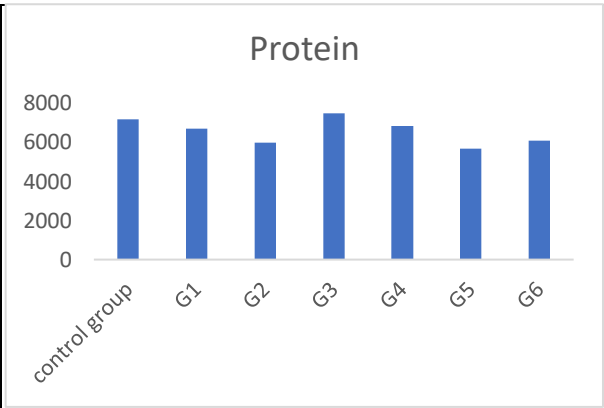

Histogram 2. Revealing the optical density values (mean±SD) of Protein materials in the brains of mice of the different experimental groups.

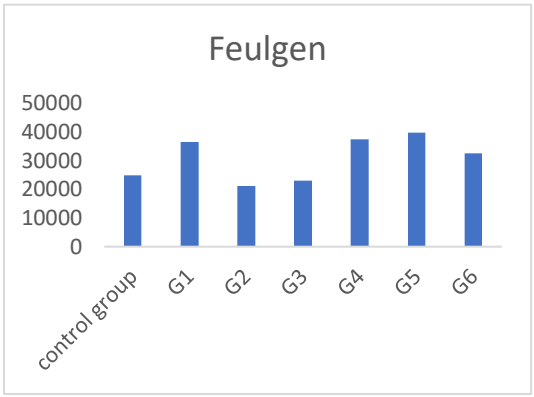

Histogram 3. Revealing the optical density values (mean±SD) of Feulgen materials in the brains of mice of the different experimental groups.

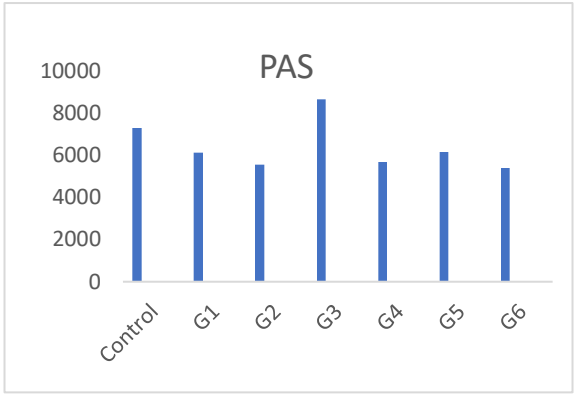

Histogram 4. Revealing the optical density values (mean±SD) of PAS +ve materials in the brains of mice of the different experimental groups.

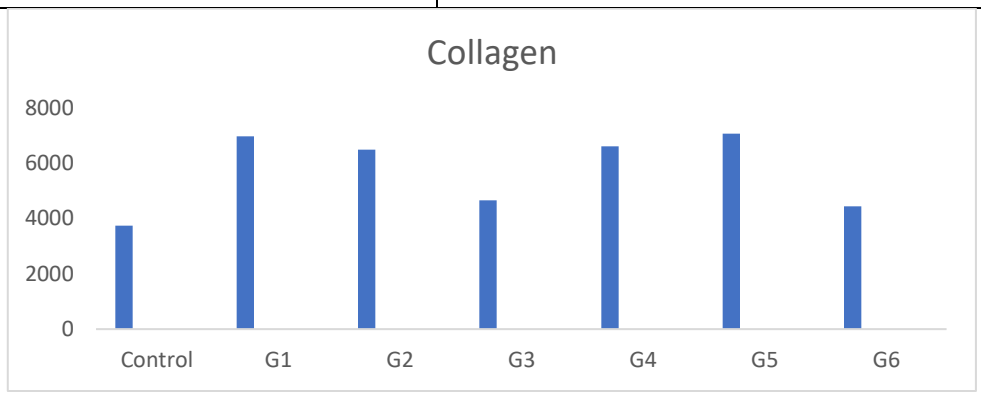

Histogram 5. Revealing the optical density values (mean±SD) of Collagen materials in the brains of mice of the different experimental groups.

DISCUSSION

Hymenolepis nana (*H. nana*), commonly known as the dwarf tapeworm, is particularly prevalent in children, with high infection rates reported in Egypt and other tropical regions. Due to their compromised immune status, children infected with *H. nana* may develop neurological symptoms, including headaches, dizziness, and seizures (Cabada et al., 2016). The neurological effects of parasitic infections often arise from the direct invasion of the CNS, as seen in cases of *Toxoplasma gondii* and African trypanosomes (Carabin & Ndimubanzi, 2011). Although the CNS lacks a conventional lymphatic system, alternative immune communication pathways exist, such as cerebrospinal fluid drainage to cervical lymph nodes (CLNs). The neurovascular unit (NVU) plays a pivotal role in maintaining CNS immune privilege by limiting leukocyte infiltration and protecting neural tissues from inflammatory damage (Bechmann & Woodroofe, 2014). However, the exact contribution of the parenchymal vasculature remains unclear, particularly in the brain. While research has shown the importance

of the brain's vasculature in delivering nutrients and oxygen, as well as removing waste products, many aspects of its function, particularly its role in metabolic homeostasis and cerebrospinal fluid (CSF) clearance, remain unclear. The relationship between meningeal vessels and immune responses remains inadequately studied (Dyrna et al., 2013). In *Toxocara canis* (*T. canis*) infections, the absence of inflammatory cell infiltration in brain tissue may result from antigen mimicry, enabling the parasite to evade immune detection. Alternatively, intrinsic CNS mechanisms may actively suppress inflammation to minimize tissue damage. This observation aligns with previous findings where *T. canis*-infected mice exhibited minimal inflammation despite a significant parasitic burden (Othman et al., 2010).

Furkuoka et al. (2003). Reported Neuropathological Lesions in Rabbits Infected with *Baylisascaris procyonis* Larva Migrans: Infected rabbits exhibited neurological symptoms such as circling, head tremors, and ataxia. Pathological analysis revealed extensive malacic lesions in the cerebellum, accompanied by astroglial proliferation, perivascular cuffing, and lymphatic infiltration. Additionally, the identification of ascarid larvae in brain tissue, specifically those measuring 65–75 μm in diameter, was reported in brain tissues (CDC, 2019).In our study, histopathological analysis of *H. nana*-infected mice demonstrated the accumulation of periodic acid-Schiff (PAS)-positive material within blood vessel walls and surrounding stroma. This finding, reminiscent of immune complex-mediated reactions observed in experimental *Schistosoma* infections, highlights a potential immunopathological response (Fu CL, et al., 2012). Astrocytes, key glial cells in the CNS, respond to injury by undergoing gliosis, a process characterized by cytokine release, protein expression changes, and structural remodeling. Recent studies suggest that viral infections may induce oxidative stress by generating reactive oxygen species (ROS), which are a contributing factor to cellular damage (Janicka et al., 2024). Understanding these mechanisms in the context of *H. nana* infection could provide valuable insights into its long-term neurological impact. Bhosale (2022) confirmed that while *H. Nana* infections are often asymptomatic; larval stages may provoke symptoms. In immunocompromised individuals, chronic infections may lead to severe CNS involvement. Revealing the optical density values of protein materials in the brains of mice from the different experimental groups (Histogram 2) recorded in immunosuppressed mice, potentially due to an increased parasitic burden.Praziquantel hepatotoxic, genotoxic, and carcinogenic properties have sparked worries despite its extensive use (Omar et al., 2005).

Growing resistance to conventional anthelmintics underscores the urgent need for alternative therapies. A recent case study by Galos et al. (2022) on plant-derived essential oils reported an atypical neurological presentation of *Hymenolepis diminuta* infection in an infant who subsequently recovered without long-term neurological sequelae. These findings highlight the intricate interplay between parasitic infections and host immune responses, underscoring the need for innovative treatment strategies. Our study highlights the challenges in detecting *H. nana* larvae in brain tissue. *Hymenolepis nana* larvae do not directly invade brain tissue; they primarily infect the small intestine. The life cycle of H. nana involves the ingestion of eggs, which hatch into oncospheres (larvae) that penetrate the intestinal villi, develop into cysticercoid larvae, and eventually mature into adult worms. While *H. nana* infection can cause intestinal inflammation and potentially lead to systemic effects, brain invasion is not a typical part of its life cycle. Brain tissue invasion by H. nana larvae is a rare and unusual occurrence (Muehlenbachs et al., 2015), as their presence is rarely observed. Future studies should focus on establishing a standardized model for investigating CNS parasitic infections. Given that some parasites exhibit erratic migration patterns, they may invade ocular or other extraneural tissues.

CONCLUSION

Histopathological alterations in the brains of infected mice were progressive and exacerbated under immunosuppressive conditions, correlating with increased cerebral parasite burden. Histochemical staining (e.g., hematoxylin and eosin) revealed significant Neuropathological changes. However, further research is needed to determine whether these alterations are directly caused by the presence of the parasite or by host immune responses to infection and treatment.

CONFLICT OF INTERESET STATEMENT

We declare that we have no conflict of interest.

REFERENCES

Bagayan M; Zongo D; Oueda A; Savadogo B. (2015). Prevalence of Hymenolepis nana among primary school children in Burkina Faso. International Journal of Medicine and Medical Sciences 7(7):125-129.DOI:10.5897/IJMMS2015.1179.

Bechmann, I., & Woodroofe, M. N., (2014). The neurovascular unit: A key component in CNS diseases. Acta Neuropathologica, 127(5), 639–662.

Bhattacharya, S. K., et al., (2003). Evaluation of praziquantel for the treatment of helminth infections. Journal of Tropical Medicine and Hygiene, 56(2), 147–152.

Cabada, M. M., & White, A. C., (2016). Treatment of microsporidiosis in children and adults: A systematic review of the literature. Clinical Infectious Diseases, 63(9), 1147–1153.

Carabin, H., & Ndimubanzi, P. C., (2011). Neurological sequelae associated with neurocysticercosis: A systematic review. PLoS Neglected Tropical Diseases, 5(5), e1051.

Carpio, A., Romo, M. L., & Parkhouse, R. M., (2018). Parasitic diseases of the central nervous system: Diagnosis and treatment. Infectious Disease Clinics of North America, 32(3), 487–505.

CDC, (2019). Toxocariasis, www.cdc.gov/parasites/. Last Reviewed: July 9, 2019, Source: National Center for Emerging and Zoonotic Infectious Diseases (NCEZID), Division of Parasitic Diseases and Malaria.

Cho, S. Y., et al., (2009). Pathophysiology and clinical features of Hymenolepiasis. Korean Journal of Parasitology, 47(Supp), S101–S110.

Dyrna, F., et al. ,(2013). The role of the blood-brain barrier in neuroinflammation. Journal of Cerebral Blood Flow & Metabolism, 33(2), 175–188.

Dyrna, F., et al., (2013). Vascular integrity and immune cell migration in the brain. Journal of Cerebral Blood Flow & Metabolism, 33(2), 175–188.

Eid, M. M., El-Kowrany, S. I., Othman, A. A., El Gendy, D. I., & Saied, E. M. (2015). Immunopathological changes in the brain of immunosuppressed mice experimentally infected with Toxocara canis. The Korean journal of parasitology, 53(1), 51. http://dx.doi.org/10.3347/kjp.2015.53.1.51.

El-Gammal, A. S., et al., 1995. Epidemiology of Hymenolepis nana infection in Egypt. Journal of Tropical Medicine and Hygiene, 98(4), 271–275.

Fu, C. L., Odegaard, J. I., Herbert, D. B. R., & Hsieh, M. H. (2012). A novel mouse model of Schistosoma haematobium egg-induced immunopathology. PLoS Pathogens, 8(3), e1002605. doi: 10.1371/journal.ppat.1002605.

Furuoka, H., Sato, H., Kubo, M., Owaki, S., Kobayashi, Y., Matsui, T., & Kamiya, H. (2003). Neuropathological observation of rabbits (Oryctolagus cuniculus) affected with raccoon roundworm (Baylisascaris procyonis) larva migrans in Japan. Journal of Veterinary Medical Science, 65(6), 695-699.

Gudissa, T., et al., (2011). The prevalence of intestinal helminths in laboratory rodents. Veterinary Parasitology, 182(3), 329–332.

Hotchkiss, R.D., (1948). A microchemical reaction resulting in the staining of polysaccharide structures in fixed tissue preparations. Archives Biocheme., 16: 131-132.

Ito, A., et al.,(1991). Experimental infections with Hymenolepis nana in murine models. Parasitology, 102(1), 43–50.

Janicka, P., Stygar, D., Chełmecka, E., Kuropka, P., Miążek, A., Studzińska, A., ... & Bażanów, B. (2024). Oxidative Stress Markers and Histopathological Changes in Selected Organs of Mice Infected with Murine Norovirus 1 (MNV-1). International Journal of Molecular Sciences, 25(7), 3614. https://doi.org/10.3390/ijms25073614.

Lversen. M. (2013). Immunosuppression for the non-transplant physician: what should you know?Breathe 9(3): 202-208; DOI: https://doi.org/10.1183/20724735.042112.

Ma, Y. H., Chen, C. Y., Chung, L. Y., Yen, C. M., Juan, Y. S., & Lin, R. J. (2022). Therapeutic effect and immune changes after treatment of Hymenolepis nana-infected BALB/c mice with compounds isolated from Leucaena leucocephala. Veterinary Sciences, 9(7), 368. doi: 10.3390/vetsci9070368.

Macnish, M. G., et al., (2001). Preparation of infective inoculum for parasitological studies. International Journal of Parasitology, 31(12), 1344–1348.

Massoud, A. M., Shazly, A. M., Shahat, S. A., & Morsy, T. A. (2007). Mirazid in treatment of human hymenolepiasis. Journal of the Egyptian Society of Parasitology, *37*(3), 863-876.

Mazia, D., Brewer, P. A., & Alfert, M. (1953). The cytochemical staining and measurement of protein with mercuric bromphenol blue. The Biological Bulletin, 104(1), 57-67.

Medeiros, R. J., et al., (2010). Use of dexamethasone in experimental models of immunosuppression. Brazilian Journal of Veterinary Research, 67(4), 345–351.

Muehlenbachs, A., Bhatnagar, J., Agudelo, C. A., Hidron, A., Eberhard, M. L., Mathison, B. A., ... & Zaki, S. R. (2015). Malignant transformation of Hymenolepis nana in a human host. New England Journal of Medicine, 373(19), 1845-1852. DOI:10.1056/NEJMoa1505892

Nessim, N. G., et al., (2000). Ethical guidelines for animal experimentation. Journal of Biomedical Research, 18(3), 235–239.

Nimmerjahn, A., et al., (2005). Resting microglial dynamics in the brain. Science, 308(5726), 1314–1318.

Omar, H. E., et al., (2005). Genotoxic and hepatotoxic effects of praziquantel in albino rats. Toxicology Letters, 158(3), 239–247.

Orozco, M. M., et al., (2018). Neurocysticercosis: An overview of its clinical presentations, diagnosis, and management. Current Opinion in Infectious Diseases, 31(5), 378–384.

Othman, A. A., et al., (2010). Toxocara canis: Neuropathological and immunohistochemical changes in experimentally infected mice. Experimental Parasitology, 126(2), 146–155.

Paolicelli, R. C., et al., (2011). Synaptic pruning by microglia is necessary for brain development. Science, 333(6048), 1456–1458.

Parija, S. C. Chaudhury A.(eds.), 2022. Hymenolepiasis ,Springer Nature Singapore Pte Ltd. (2022), 4.Bhosale NK,Hymenolepiasis ,Chapter· September 2022 S. C. Parija, A. Chaudhury (eds.), Textbook of Parasitic Zoonoses, Microbial Zoonoses, https://doi.org/10.1007/978-981-16-7204-0_36.

Pearse, A.G., (1977). Histochemistry, Theoretical and Applied. 3rd ed., Livingstone, C., London. p.1.

Pinto, P. S., et al. ,(1994). Prevalence of Hymenolepis species in rodents from urban areas. Parasitology Research, 80(2), 127–131.

Reedy, C. L. (2006). Review of digital image analysis of petrographic thin sections in conservation research. Journal of the American Institute for Conservation, 45(2), 127-146. https://doi.org/10.1179/019713606806112531.

Ribble, D., et al.,(2005). Apoptosis and necrosis: Detection and analysis. Biotechnology, 39(1), 1–8.

Schafer, D. P., et al., (2013). Microglia sculpt postnatal neural circuits in an activity- and complement-dependent manner. Neuron, 74(5), 691–705.

Sheehan, D.C. and Hrapchak, B.B.,(1980). Theory and Practice of Histotechnology. 2nd ed., Mosby, St. Louis (MO), London, pp: 177-178.

Suvarna, S. K., et al.,(2013). Bancroft's Theory and Practice of Histological Techniques. 7th Edition. Churchill Livingstone.

Tremblay, M. È., et al., (2010). Microglial interactions with synapses and their role in neural plasticity. Neuron, 69(1), 10–18.

Valle, S. (1986): Special stains in microwave oven. J. Histotechnol., 9:237-248.

Van Riet, E., Hartgers, F. C., & Yazdanbakhsh, M. (2007). Chronic helminth infections induce immunomodulation: Consequences and mechanisms. Immunobiology, 212(6), 475–490.

World Health Organization (WHO), (2013). Helminth control in school-age children: A guide for managers of control programs. Geneva: WHO Press.